77
6-24-77
25 cys. to NTIS

UCID- 17494

Lawrence Livermore Laboratory

MODAL ANALYSIS OF THE NRC PRESSURE SUPPRESSION EXPERIMENTAL FACILITY

Michael R. Posehn

May 20, 1977

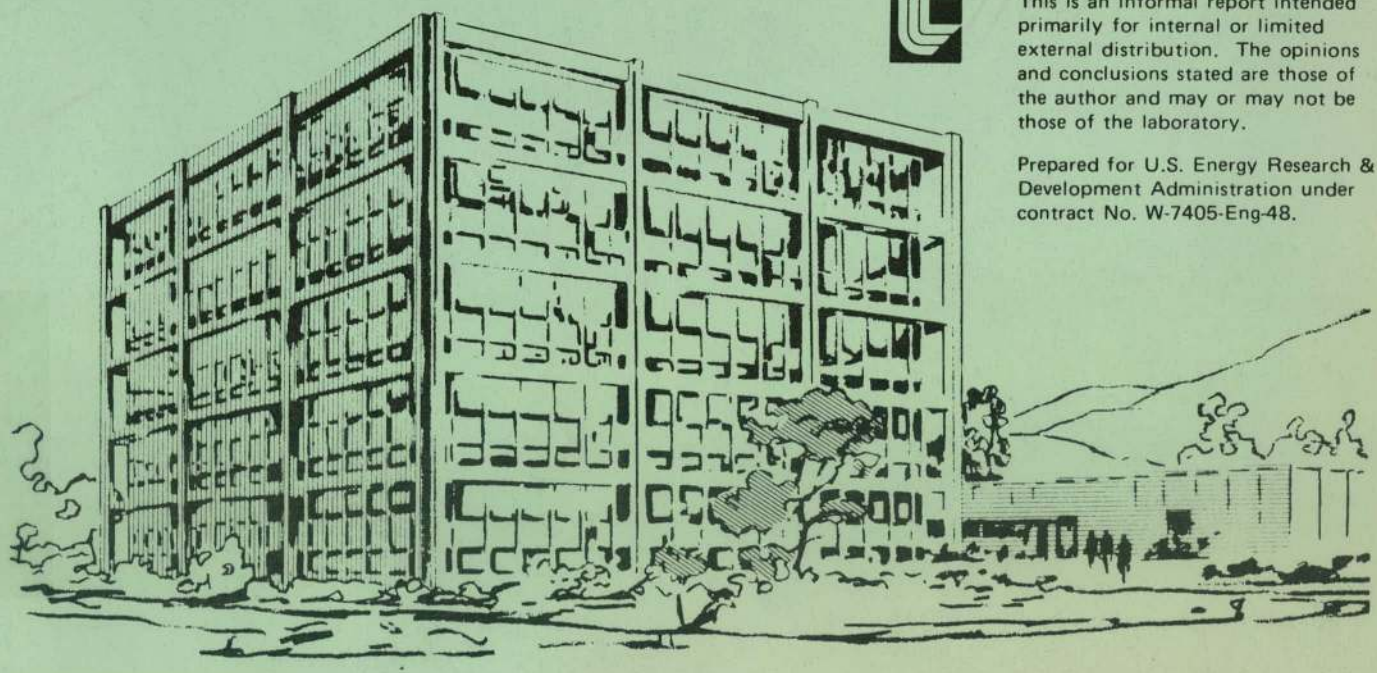

Prepared for U.S. Energy Research & Development Administration under contract No. W-7405-Eng-48.

DISCLAIMER

CONTENTS

ABSTRACT

The 1/5th scale model Mark I pressure suppression facility was experimentally analyzed in order to determine its fundamental modes of vibration. The results of the modal analysis revealed seven apparent modes with frequencies below 100 Hz. In this report each mode is characterized by a description of the motion, the natural frequency, and the response amplitude. The results indicate that the response of the torus to an impulsive load in the vertical direction is dominated by two modes at 12.2 Hz and 59.8 Hz.

INTRODUCTION

The NRC pressure suppression experimental facility is a 1/5th scale model of a Mark I boiling water reactor (BWR) containment system. In a Mark I BWR the reactor is surrounded by a dry well having the general shape of an incandescent bulb. Vent pipes lead from the dry well into a toroidal wet well that surrounds the dry well. Following a loss-of-coolant accident (LOCA), a steam pipe break within the dry well, the air and steam pass through the vent pipes into a ring header inside the toroidal wet well and then through a set of down-comer pipes into a pool of water. The 1/5th scale model consists of a 90° segment and a 7.5° segment of the toroidal wet well. Experiments are being conducted with the scale model in order to predict the dynamic behavior of a full-scale Mark I pressure suppression system during a LOCA.

Since the dynamic behavior of the scale model is of primary importance, a modal analysis of the assembly was performed in order to determine its fundamental modes of vibration. A conceptual mathematical model of the torus was used in order to select appropriate locations for the application of low-level impulsive loads. The impulsive loads were created by impacting the torus with an instrumented sledge hammer, and the hammer force and resulting torus motion were recorded using the TDAC [1] computer system. The torus was subjected to two series of impacts, vertical and horizontal, for two configurations, partially filled with water* and empty. Modal analysis theory was then used to combine the experimental data with the conceptual model to reveal the natural frequencies and mode shapes of seven apparent modes of vibration below 100 Hz. This report presents a brief explanation of modal analysis theory and illustrates how this theory was applied to the torus assembly.

Modal Analysis

Although modal analysis is primarily an experimental technique, it is essential to construct a conceptual mathematical model of the structure to be analyzed. The model is used to select impact locations on the structure and to aid in the interpretation of the results. If the structure cannot be discribed by a model of the proper form, then the analysis cannot be applied with confidence. Specifically, modal analysis can be applied to any system that can be described by a set of simultaneous second-order linear differential equations of the form

* Water level 2.4 in. below centerline.

$$M\ddot{x}(t) + C\dot{x}(t) + kx(t) = f(t) \tag{1}$$

where

$f(t)$ = force vector

$x(t)$ = displacement vector

$\dot{x}(t)$ = velocity vector

$\ddot{x}(t)$ = acceleration vector

and M, C, and K are the mass, damping, and stiffness matrices. If the system has n degrees of freedom, then the vectors are n-dimensional and the matrices are n x n. Solutions of the homogeneous equation describe the n different modes of vibration of the system. Modal analysis can be used to compute the M, C, and K matrices from experimental data. Once these matrices are known, it is possible to calculate the response of the system to any arbitrary driving force vector using Equation 1.

General Theory

It is necessary to review the theory in order to illustrate how impact locations are determined and how the mode shapes can be computed. First, we will briefly describe some properties of the solutions of the homogeneous form of Equation 1. Taking the Laplace transform of equation (1) gives:

$$B(s)X(s) = F(s) \tag{2}$$

where

$F(s)$ = Laplace transform of the force vector

$X(s)$ = Laplace transform of the displacement vector

$B(s) = Ms^2 + Cs + K$ = the system matrix

s = the Laplace variable.

The transfer matrix is defined as the inverse of the system matrix

$$H(s) = B(s)^{-1} \tag{3}$$

which implies that

$$X(s) = H(s)F(s). \tag{4}$$

Therefore, the transfer matrix is an n x n matrix

$$H(s) = \begin{bmatrix} h_{11}(s) \cdots\cdots\cdots h_{1n}(s) \\ \cdot \\ \cdot \\ \cdot \\ h_{n1}(s) \cdots\cdots\cdots h_{nn}(s) \end{bmatrix} \tag{5}$$

where $h_{ij}(s)$ is the transfer function that specifies the response of the $i^{\underline{th}}$ element due to the force applied at the $j^{\underline{th}}$ element. Since the elements of B(s) are quadratic functions of the Laplace variable s, the elements of H(s) are ratios of polynomials in s; i.e.,

$$h_{ij}(s) = \frac{b_0+b_1s+....+b_{2n}s^{2n}}{\det(B(s))} \tag{6}$$

where the b's are polynomial coefficients and det (B(s)) is a polynomial of order 2n. If the roots of det (B(s)) are distinct, then H(s) can be written as

$$H(s) = \sum_{k=1}^{2n} \frac{a_k}{s-p_k} \tag{7}$$

where

a_k = the residue matrix for the $k^{\underline{th}}$ root
p_k = the $k^{\underline{th}}$ root of det (B(s)) or $k^{\underline{th}}$ pole of H(s).

If the system is subcritically damped, the roots occur in complex conjugate pairs of complex numbers,

$$p_k = -\sigma_k + i\omega_k, \; p_k^* = -\sigma_k - i\omega_k \tag{8}$$

where σ_k is the damping coefficient and ω_k is the natural frequency. For each pole there is a corresponding modal vector u_k which is a solution of the equation,

$$B(p_k)u_k = \emptyset \tag{9}$$

Using the modal vectors, the transfer matrix can be written in terms of the n complex conjugate pairs of poles

$$H(s) = \sum_{k=1}^{n} \frac{u_k u_k^t}{s-p_k} + \frac{u_k^* u_k^{*t}}{s-p_k^*} . \tag{10}$$

Each term in the summation is an n x n complex matrix that corresponds to the contribution of each mode to the transfer matrix.

It can be shown [2-5] that using (10) each row and column of the residue matrix contains the same modal vector multiplied by a component of itself. Therefore, the modal vectors and pole locations can be computed from any row or column of the transfer matrix. This means that a structure can be analyzed

by exciting it at each point and measuring the response at one point, identifying a column, or by exciting it at one point and measuring the response at every point, identifying a row.

When the modal vectors are real-valued, then they are equivalent to the mode shape. In the case of complex modal vectors, the mode shape can be computed from the magnitude of the residue.

Torus Conceptual Model

Since the purpose of the analysis was to identify the rigid-body modes of vibration of the torus assembly, a simplified model was considered. The torus was divided into a beam composed of seven lumped masses, as shown in Fig. 1. The first, fourth, and seventh masses are located at flange joints, and the other four masses correspond to weld-joint locations. The center of the torus is constrained in the X direction by a steel beam, and both the center and end are supported by load cells.

Translational motion of the model in the X- and Z-axes can be described by a set of fourteen simultaneous differential equations. Therefore, all of the modes of vibration of the model can be identified by measuring the response of the system to seven X-axis impacts and seven Z-axis impacts. Since the motion of each mass is measured relative to its at-rest position, it is not necessary to consider the curvature of the torus. The X-axis and Y-axis in Fig. 1 correspond to the radial and the tangential directions of the torus.

IMPACT DATA

Equipment

The modes of vibration were excited by impacting the structure with a 2.5 kg hammer. A polyurethane cap was used on the hammer to cushion the impact sufficiently to excite only those modes with frequencies below 100 Hz. The impact force was measured with a quartz force transducer mounted between the cap and the hammer head, and the transducer output was fed through a charge amplifier. Two geophones were used to measure the response of the structure in the radial and vertical directions. The geophones respond to vibrations above 1 Hz with a sensitivity of approximately 0.5 V/mm/s. The geophone output did not require any amplification. All transducers were accurately calibrated before they were used. The transducer signals were recorded using a

portable analog tape system, and then the tapes were played back and digitized using the TDAC computer system. During the digitizing process the analog signals were amplified by a factor of 100, filtered at 250 Hz (8-pole Bessel) and sampled at 1000 Hz. This choice of sampling parameters allowed accurate analysis of frequencies up to 100 Hz.

Since the TDAC computer system is transportable, it is usually not necessary to use the intermediate step of recording the data on analog tape. However, it was used in this case, since there was not a sufficient amount of sheltered space at the site to house the computer.

Procedure

Figure 2 is a top view of the torus that shows the impact points and transducer locations for both the horizontal and vertical impact series. The two transducers provided a record of the resulting motion in the X and Z directions, where Z is vertical. The seven impact points were thought to be sufficient to excite the major rigid-body modes of vibration. Each impact point was struck three times with the hammer, and each time the response was collected for 4 seconds after impact. This was the amount of time necessary for the vibrations to decay to the ambient noise level.

Figure 3 is a plot of the hammer force for a typical impact; in this case it is for a vertical impact at location 1. The waveform is a 2860 Newton half-sine pulse with a duration of approximately 0.075 seconds. Figures 4a and 4b show the velocity responses in the Z- and X-axes for the same vertical impact. Both response waveforms appear to be composed of a high-frequency component which decays rapidly and a low-frequency component of approximately 12 Hz.

Data Reduction

The first step in the data reduction process was to convert the velocity data into acceleration. This was accomplished by using a five-point numerical differentiation algorithm. Figures 5a and 5b show typical Z- and X-axis data after differentiation. An average transfer function was then computed for each pair of impact locations and response directions.

First the force auto-spectral density and force-response cross-spectral density were computed for each impact,

$$G_{F_iF_i} = F_iF_i^* \tag{11}$$

and

$$G_{X_jF_i} = X_jF_i^* \tag{12}$$

where * denotes the complex conjugate and

F_i = the Fourier transform of the impact force

$G_{F_iF_i}$ = the force auto-spectral density

X_j = the Fourier transform of the response

$G_{X_jF_i}$ = the cross-spectral density

i = the index of the impact point

j = the index of the response point

The auto- and cross-spectral densities were then average for the three impacts at each location, and the transfer functions were computed from the equation

$$g_{ij} = s^2h_{ij} = \frac{G_{X_jF_i}}{G_{F_iF_i}} \tag{13}$$

where

$G_{X_jF_i}$ = the average cross-spectral density

$G_{F_iF_i}$ = the average force auto-spectral density

h_{ij} = the transfer function from force to displacement

g_{ij} = the transfer function from force to acceleration.

The responses from the fourteen impacts combined with Equation 13 are sufficent to specify one row of the transfer matrix. The computer program required to compute the mass, stiffness, and damping matrices of Eqaution 1 is under development at this time; however, with certain assumptions, the mode shapes can be computed directly from the transfer function data.

RESULTS

90° Torus Assembly

Figures 6a and 6b are simultaneous plots of the transfer function amplitude in g's/Newton for all seven vertical impacts. Likewise, Figs. 7a and 7b show the amplitudes for the horizontal impacts. Several modes are indicated by the coincident peaks in amplitude and the characteristics of seven of these are summarized in Table 1. The table includes a brief description of the type of motion, the natural frequency when partially filled with water and when empty, and the response amplitude for both vertical and horizontal impacts. The amplitude is equivalent to the peak response of the torus for a sinusoidal 1 kilonewton driving force at the resonant frequency.

For simple modes that are lightly damped and well separated, the imaginary parts of the complex transfer functions can be used to construct the mode shapes. With this assumption, the mode shapes for the seven dominant modes were computed and are shown in Figs. 8 through 14. Each figure shows the displacement of the torus from three different views; however, the displacements are not necessarily scaled equally for each view.

Modes 1 and 2 appear to have the same motion (see Figs. 8 and 9). This may be due to coupling with orbital motion about the Y-axis which, unfortunately, is not observable with this data. The response amplitudes indicate that both of these modes are excited primarily by horizontal forces.

Again, modes 3 and 4 appear to be very similar; however, mode 3 at 12.2 Hz is clearly dominant. The amplitude indicates that it can be excited significantly by both horizontal and vertical forces.

A fifth mode appears to be the first bending mode of the torus as if it were a simple beam. This mode does not appear in the response to horizontal impacts, and it contributes little to the vertical impact response.

There is another pair of modes, number 6 at 59.8 Hz and number 7 at 61.8 Hz which have very similar motions. Number 6, along with number 3, dominate the response to vertical impacts.

7.5° Torus Segment

The 7.5° torus segment was struck at four locations in order to determine its fundamental natural frequencies. Figure 15 shows the four impact locations and the three measurement directions. The structure was struck in the X-direction at two locations in order to determine the first torsional mode. Table 2 summarizes the modes that were identified. Three modes appear in the X-axis data. The first mode corresponds to X-axis translation and the second mode is due to torsion of the segment relative to its supports. Although the shape of the third mode cannot be specified from data at only two points, its frequency was apparent at 80 Hz. Unfortunately, no information was obtained for the Y-axis motion due to an instrumentation failure. The fundamental frequency in the Z-axis appeared to be approximately 50 Hz.

CONCLUSIONS

The natural frequencies of seven modes of vibration of the torus assembly have been identified by analyzing the structural response to a series of hammer impacts. In addition, the mode shapes at those frequencies were also computed with the assumption that the modes were slightly damped and well separated. The results indicate that the torus dynamics are dominated by modes at 12.2 and 59.8 Hz; however, in both cases the response amplitude is less than 1.0 g/kilonewton.

REFERENCES

1. Fisher, D. K., Posehn, M. R., Sindelar, F. L., Bell, H. H., "Computer-Based Transportable Data-Acquisition and Control System," 45th Shock and Vibration Symposium, Albuquerque, New Mexico, Oct. 19-21, 1976

2. Potter, R., "A General Theory of Modal Analysis for Linear Systems," The Shock and Vibration Digest, Vol 7, No. 11, Nov. 1975

3. Klosterman, A. and Zimmerman, R., "Modal Survey Activity via Frequency Response Functions," SAE National Aerospace Engineering and Manufacturing Meeting Paper #751068, Nov. 1976

4. Klosterman, A., McClelland, W. A. and Sherlock, J. E., "Dynamic Simulation of Complex Systems Utilizing Experimental and Analytical Techniques," ASME 75-WA/Aero-9

5. Richardson, M. and Ramsey, K. A., "Making Effective Transfer Function Measurements for Modal Analysis," Proceedings of the Institute of Environmental Sciences, 1976

TABLE 1 - MODAL ANALYSIS RESULTS ON THE 1/5 SCALE 90° TORUS ASSEMBLY

Mode	Description of the Motion	Natural Frequency		Response Amplitude g/kN			
				Vertical Impact		Horizontal Impact	
		Filled	Empty	Vertical	Horizontal	Vertical	Horizontal
1	Horizontal Rotation	5.0	5.0	-	0.040	0.006	0.150
2	Horizontal Rotation	8.0	8.0	-	0.025	0.009	0.110
3	Vertical Rotation + Vertical Translation + Horizontal Rotation	12.2	12.7	0.410	0.180	0.200	0.073
4	Vertical Translation + Horizontal Rotation + Horizontal Translation	13.9	14.5	0.095	0.085	0.100	0.170
5	Vertical Bending	25.9	27.5	0.075	0.040	0.018	-
6	Vertical Translation + Horizontal Translation	59.8	64.9	0.210	0.900	0.060	0.230
7	Vertical Translation + Horizontal Rotation	61.8	74.0	0.084	-	0.080	0.230

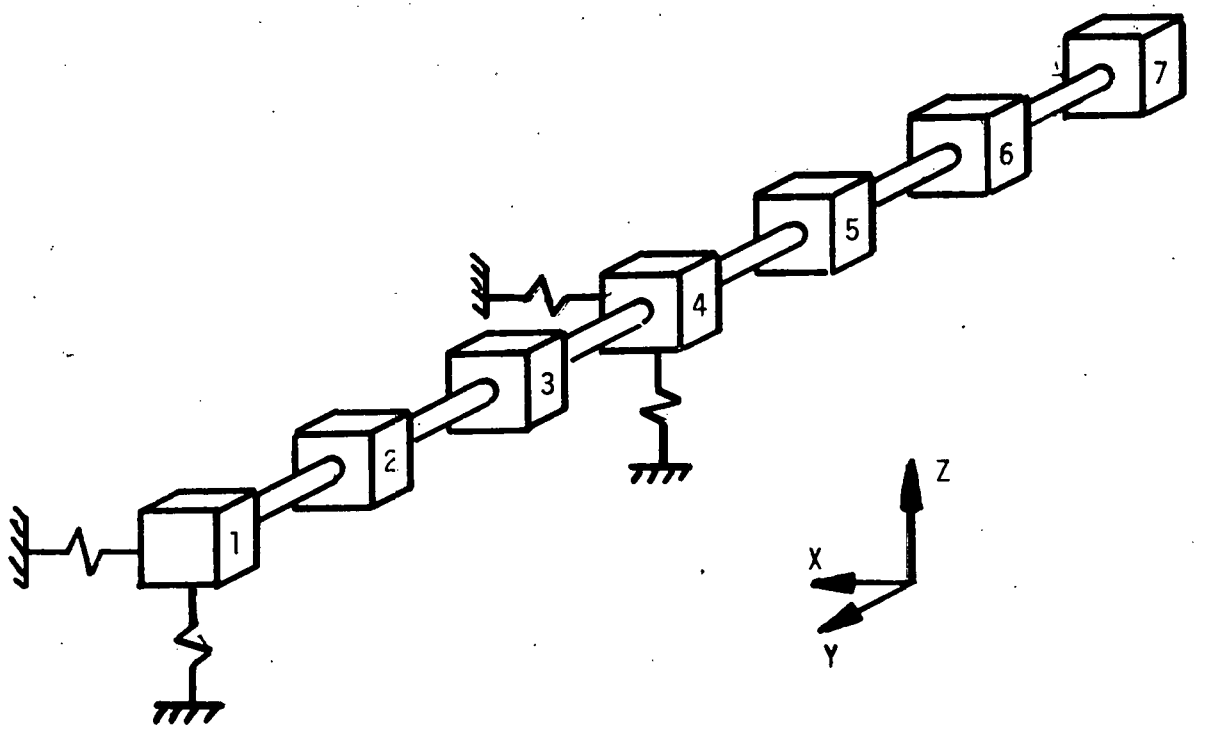

Figure 1 - A Lumped-Mass Model of the 90° Torus Segment

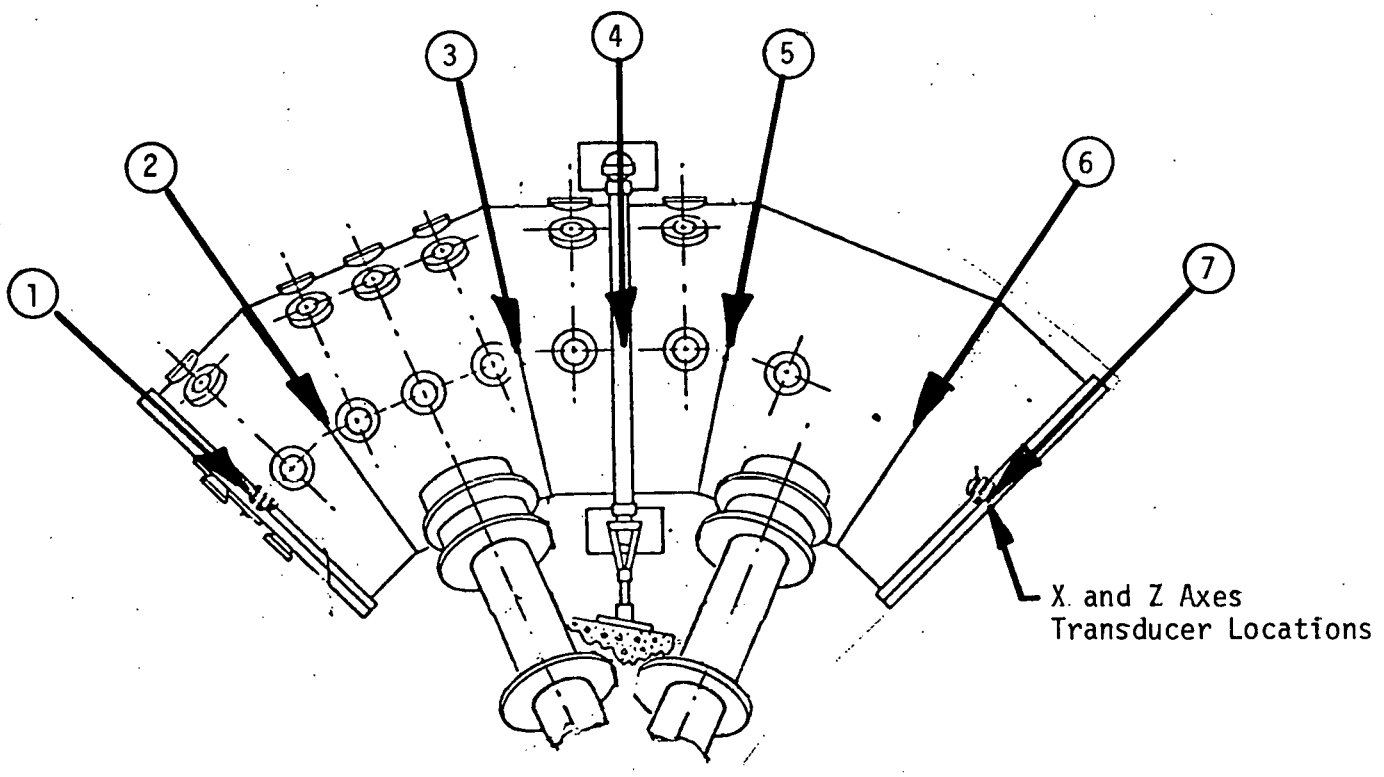

Figure 2a - Vertical Impact Locations

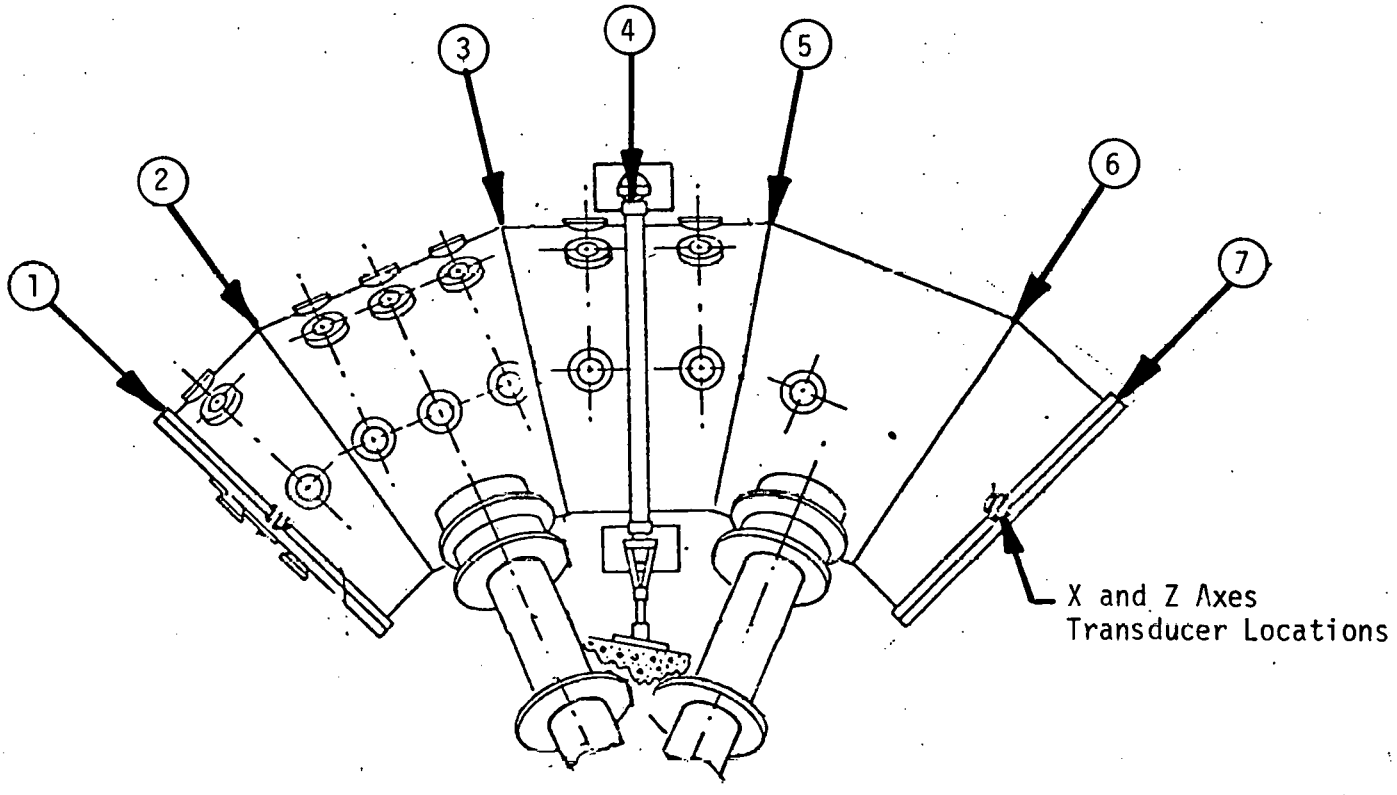

Figure 2b - Horizontal Impact Locations

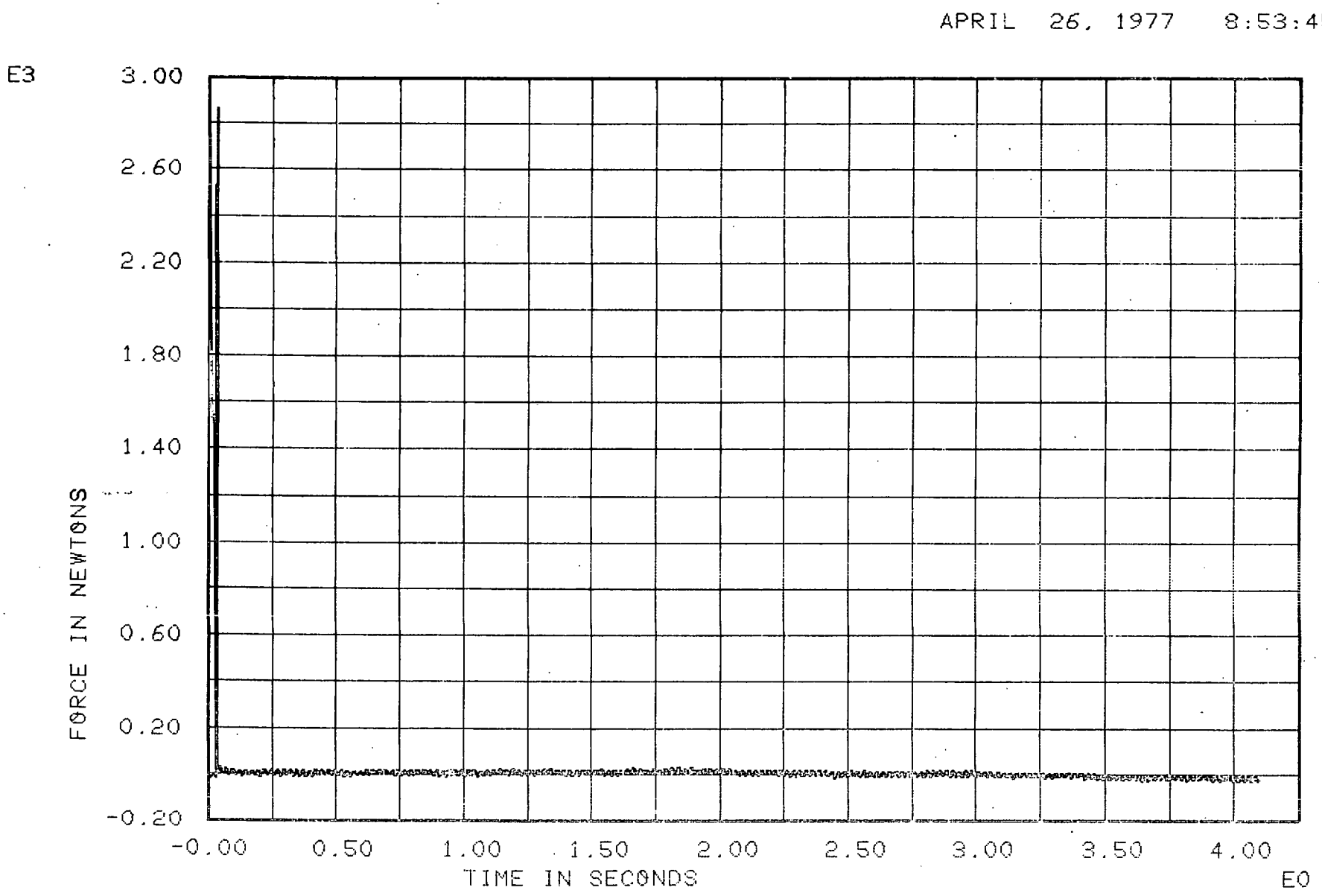

Figure 3 - Hammer Force Wave Form for a Vertical Impact at Location 1.

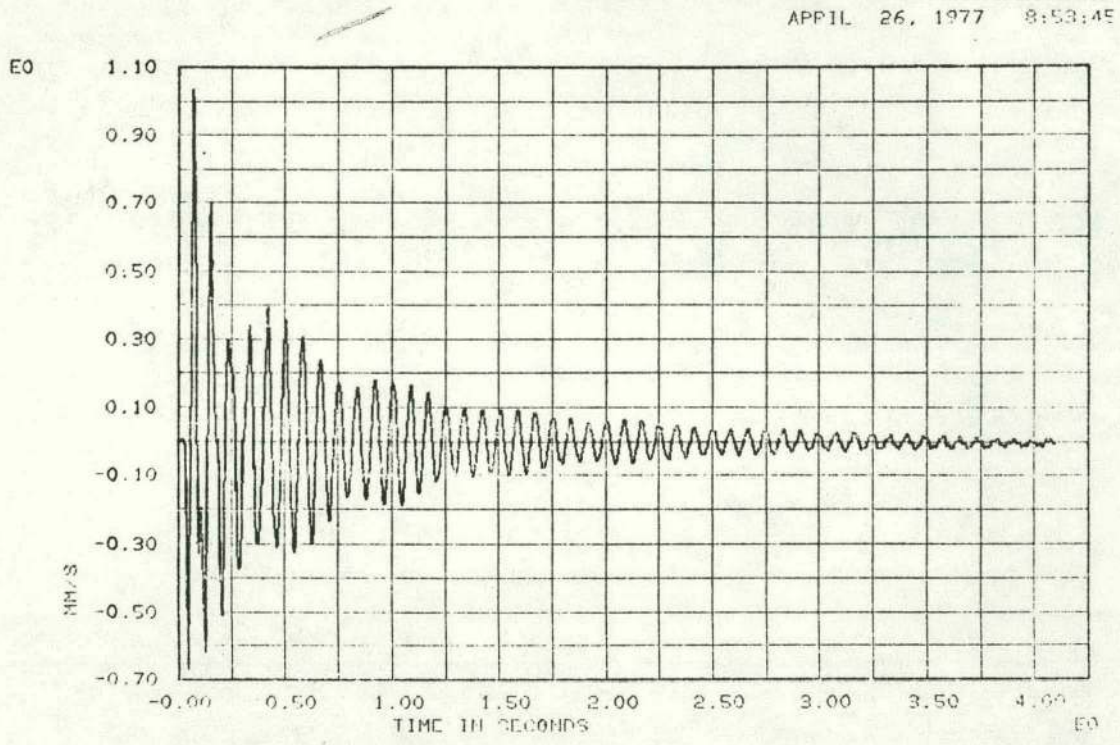

Figure 4a - Z-Axis Velocity Response at Location 7 for a Vertical Impact at Location 1.

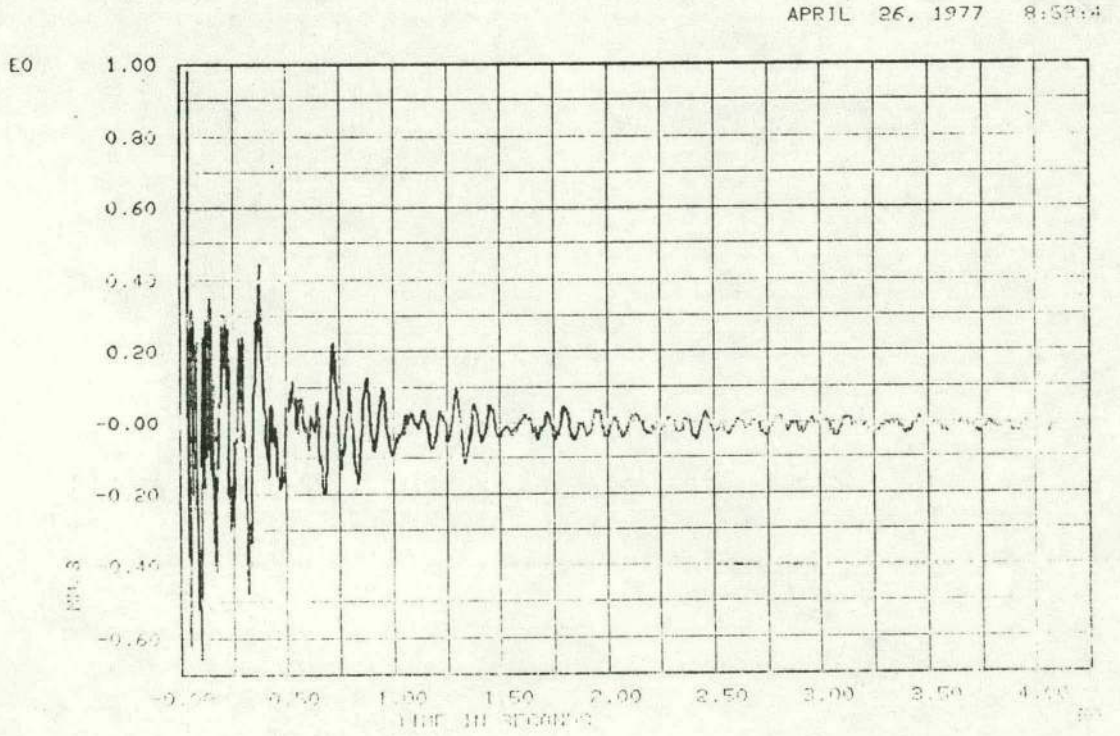

Figure 4b - X-Axis Velocity Response at Location 7 for a Vertical Impact at Location 1.

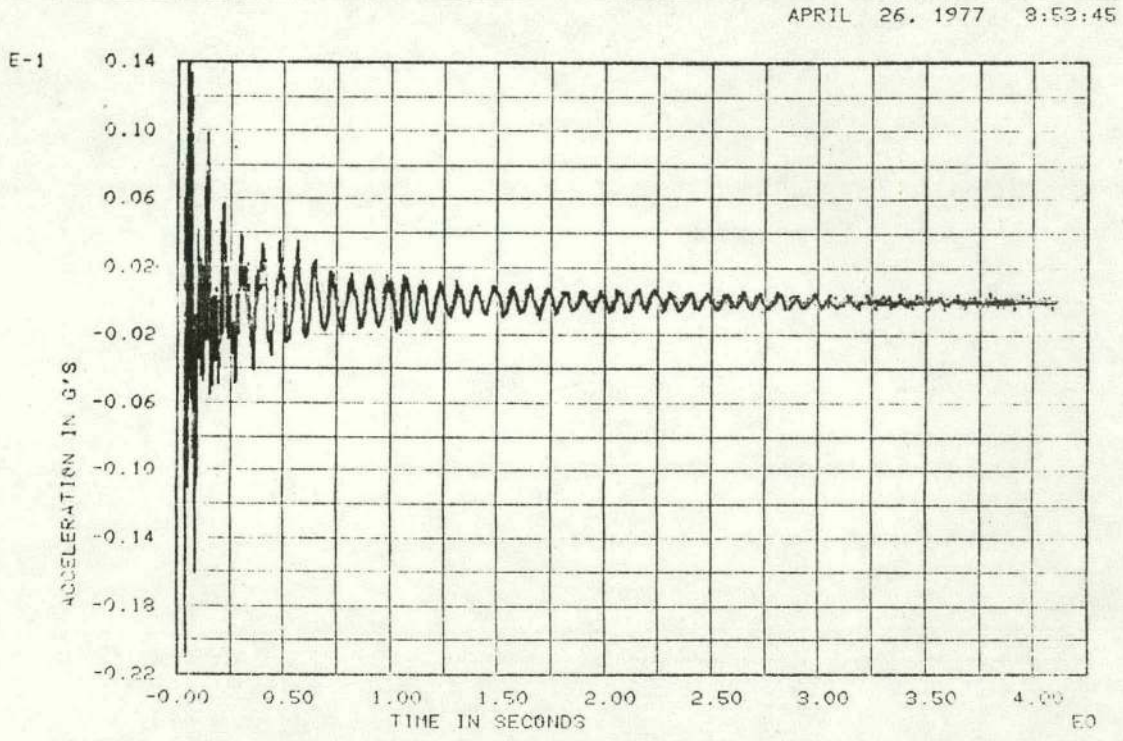

Figure 5a - Computed Z-Axis Acceleration Response at Location 7 for a Vertical Impact at Location 1.

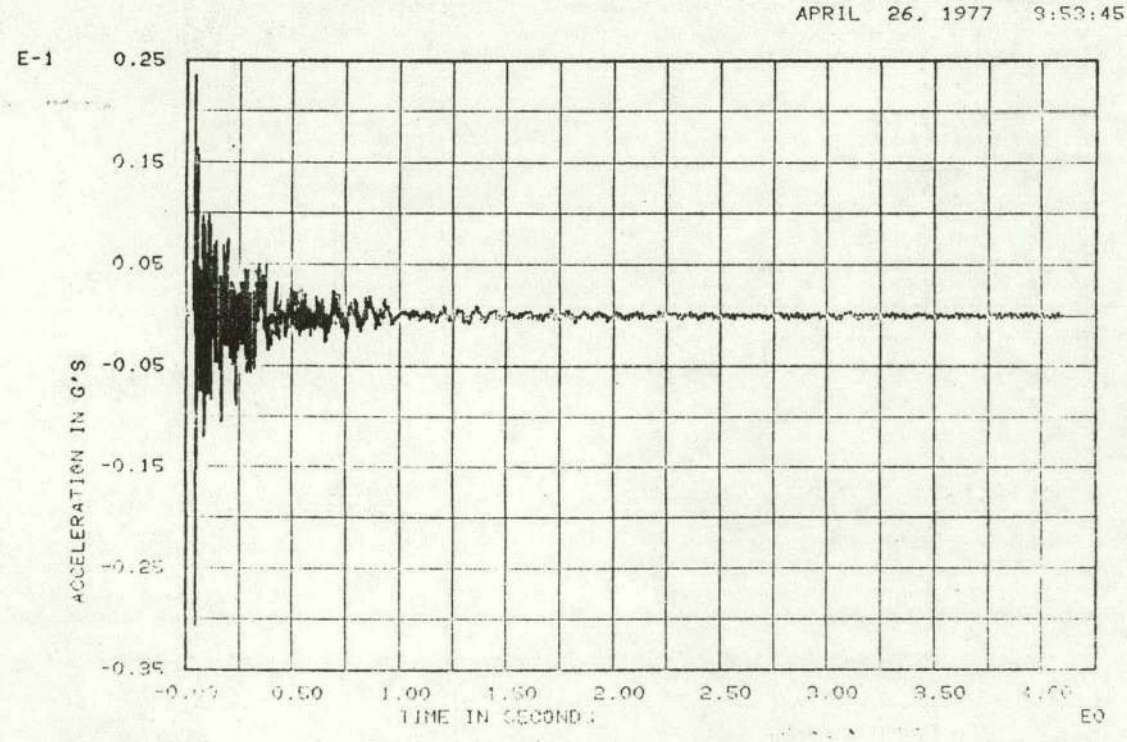

Figure 5b - Computed X-axis Acceleration Response at Location 7 for a Vertical Impact at Location 1.

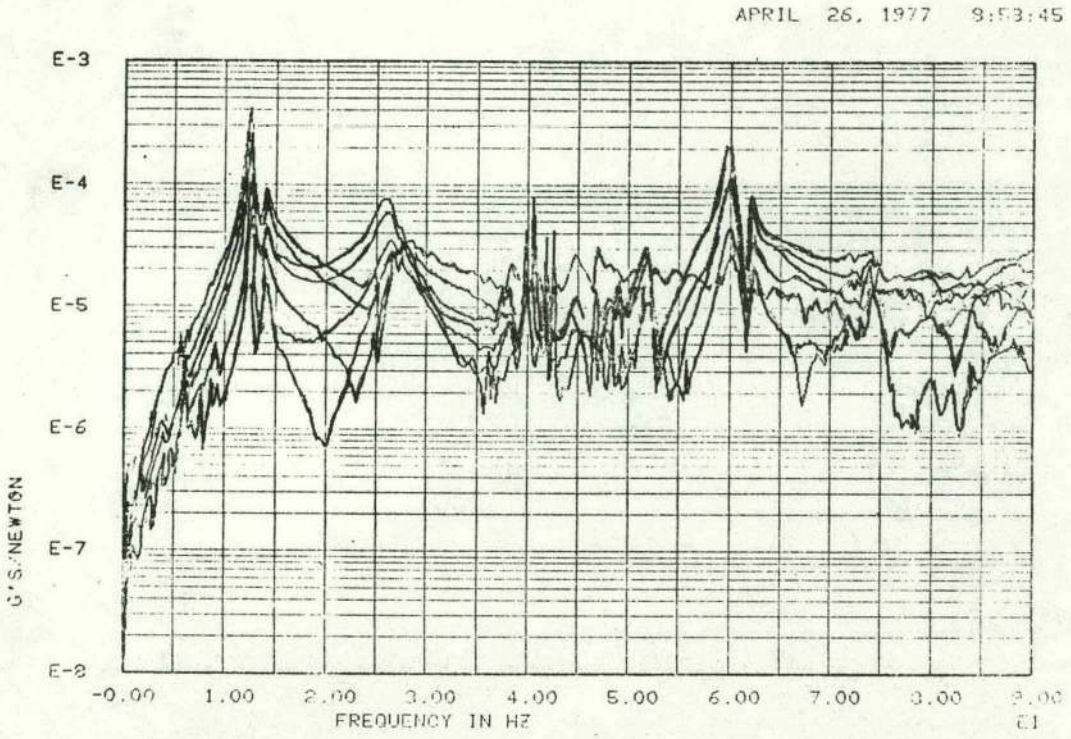

Figure 6a - Absolute Value of the Z-Axis Transfer Functions for Seven Vertical Impacts.

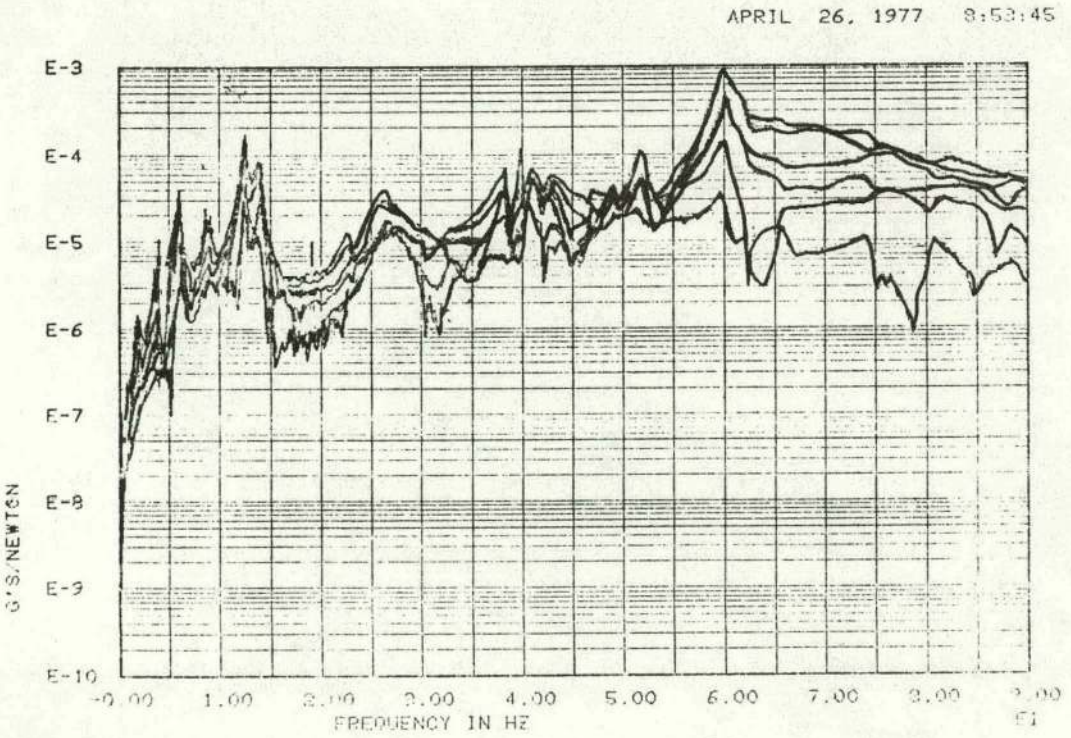

Figure 6b - Absolute Value of the X-Axis Transfer Functions for Seven Vertical Impacts.

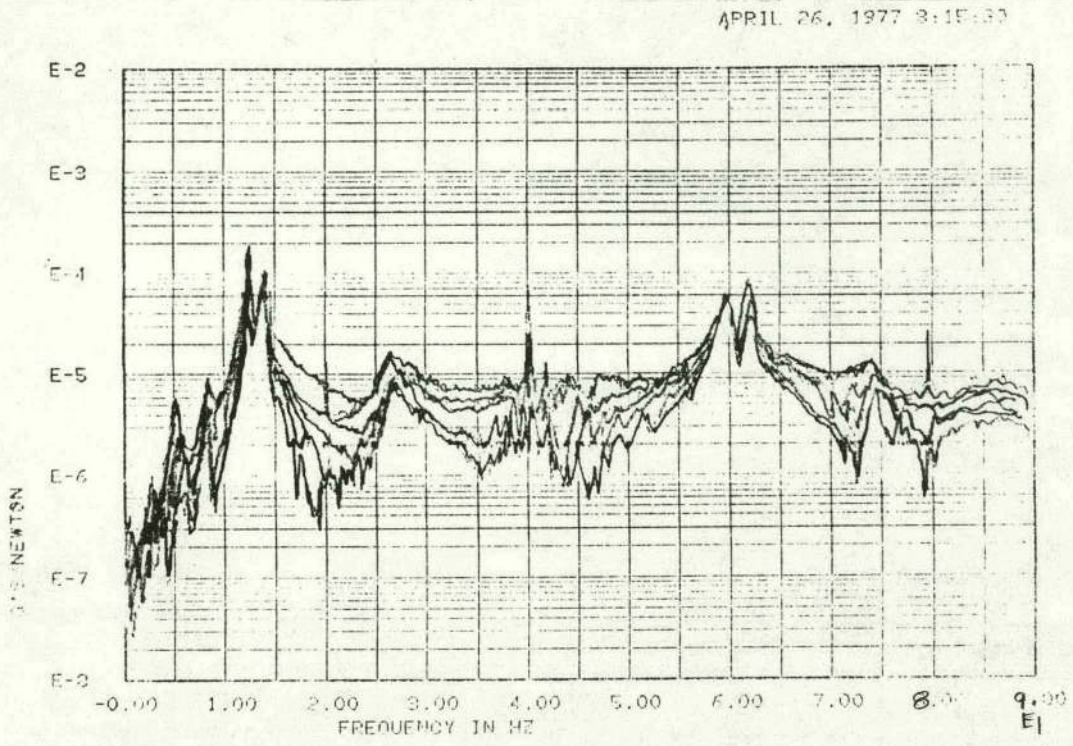

Figure 7a - Absolute Value of the Z-Axis Transfer Functions for Seven Horizontal Impacts.

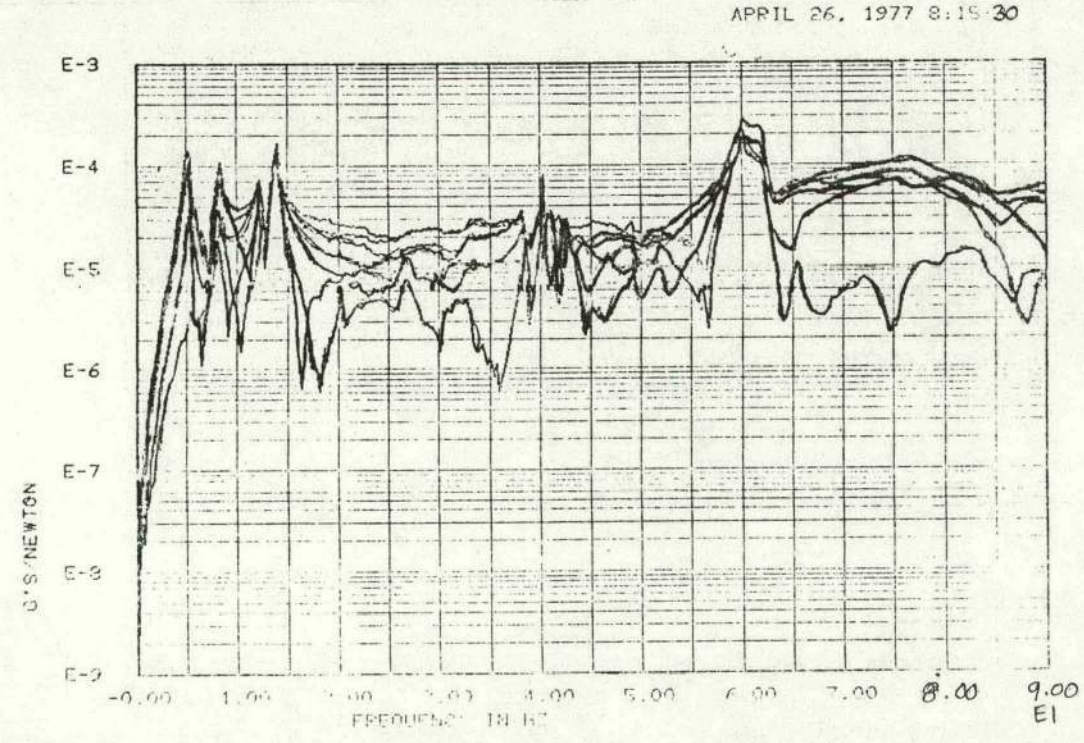

Figure 7b - Absolute Value of the X-Axis Transfer Functions for Seven Horizontal Impacts.

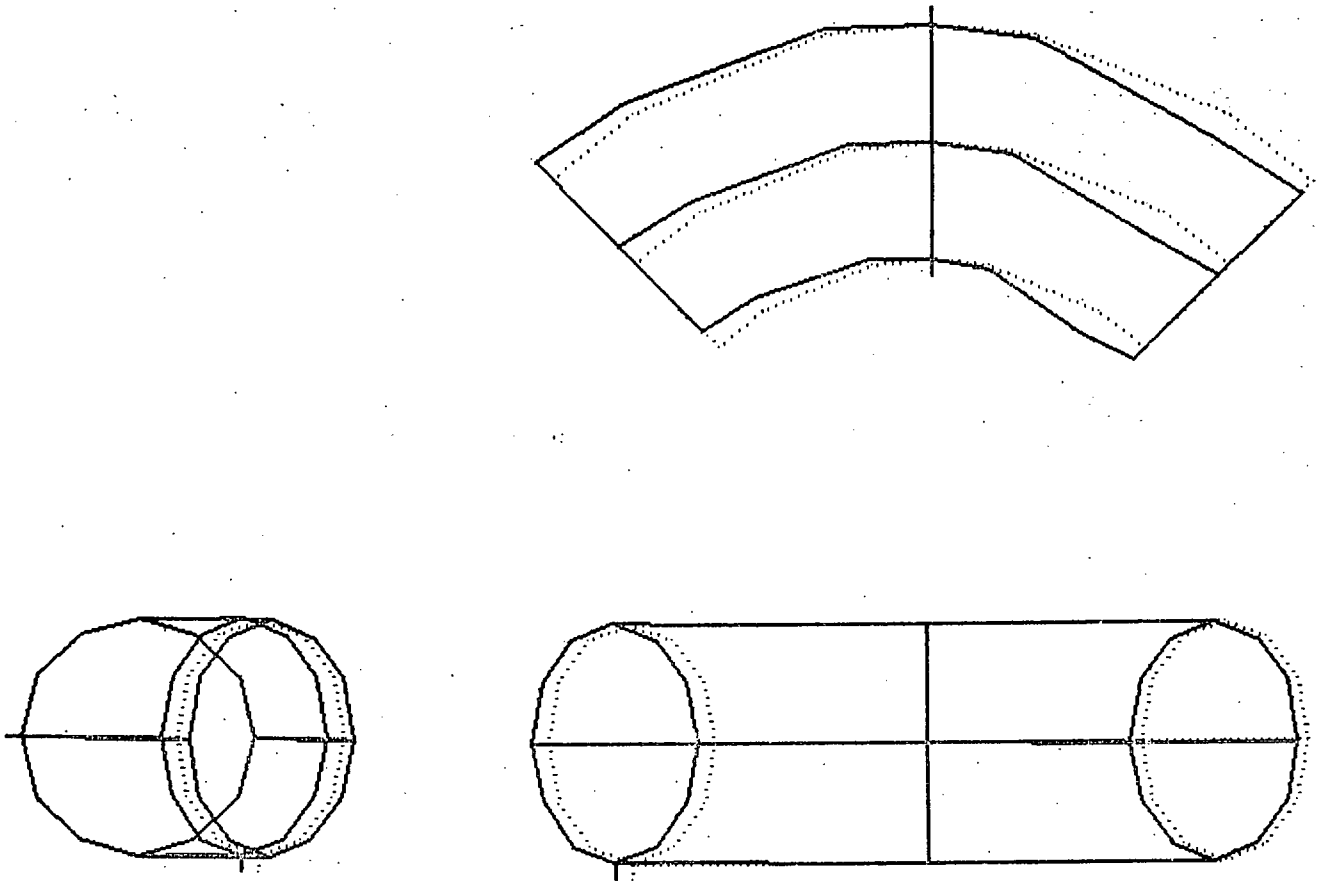

Figure 8 - Mode #1, 5 Hz.

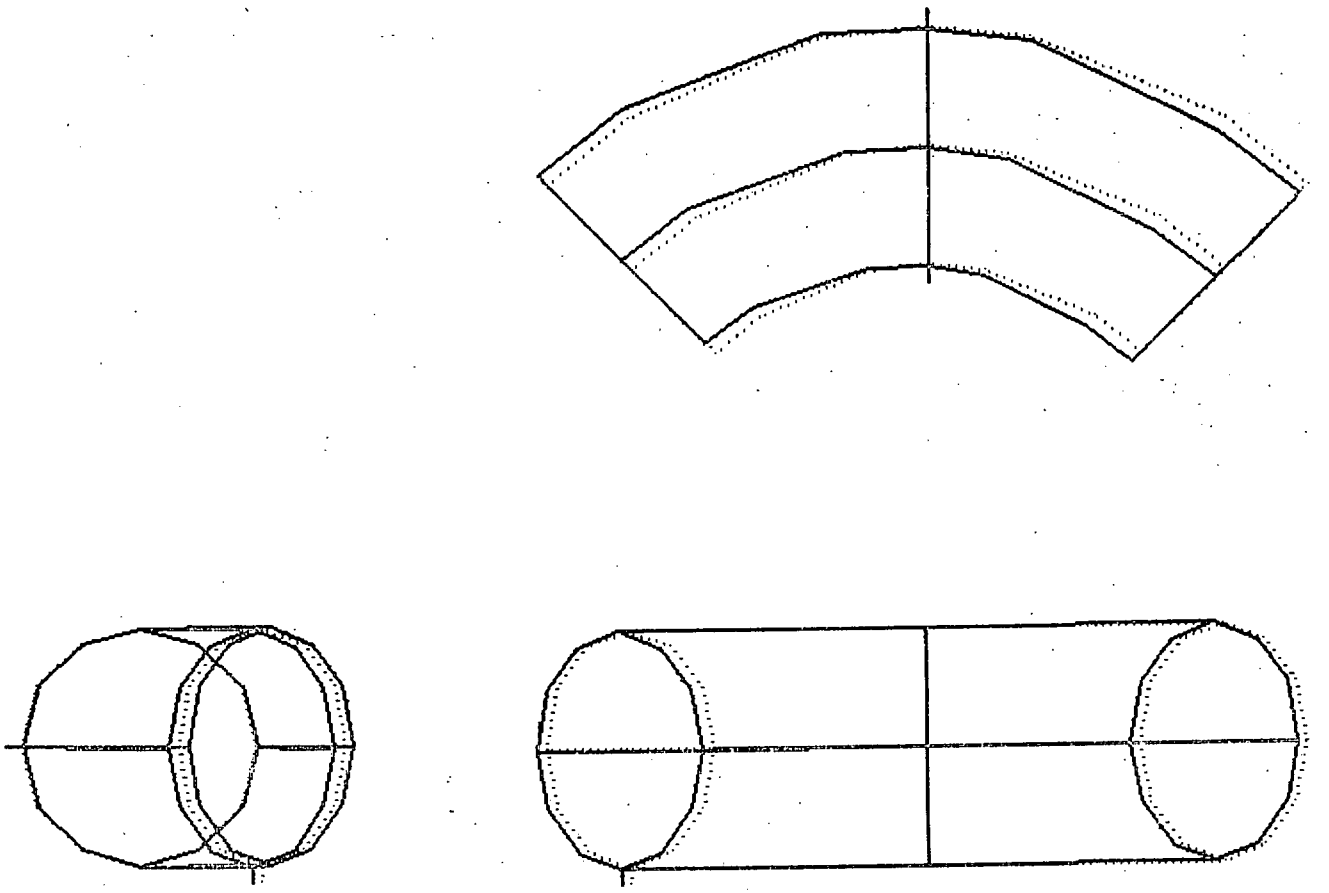

Figure 9 - Mode #2, 8 Hz.

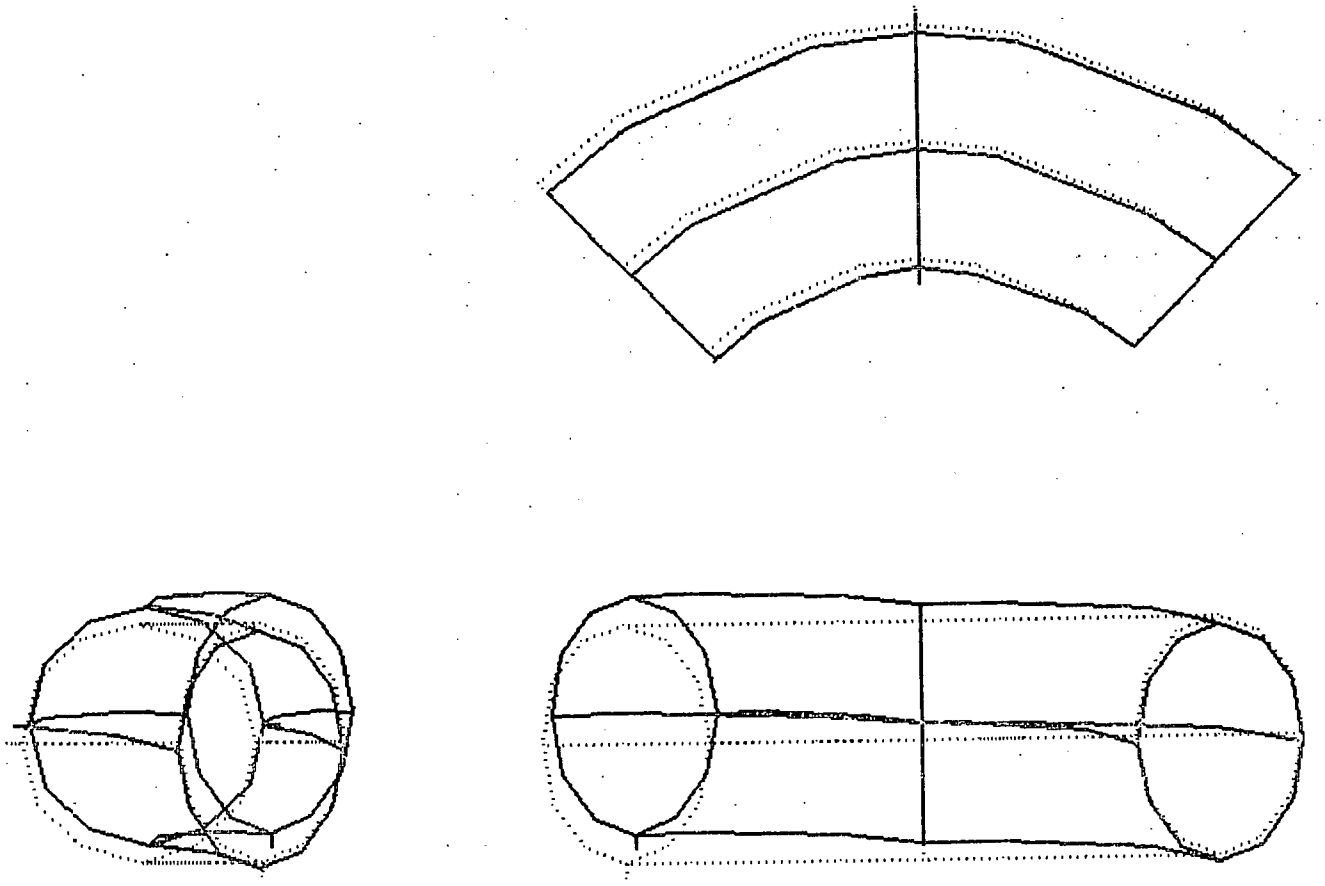

Figure 10, Mode #3, 12.2 Hz.

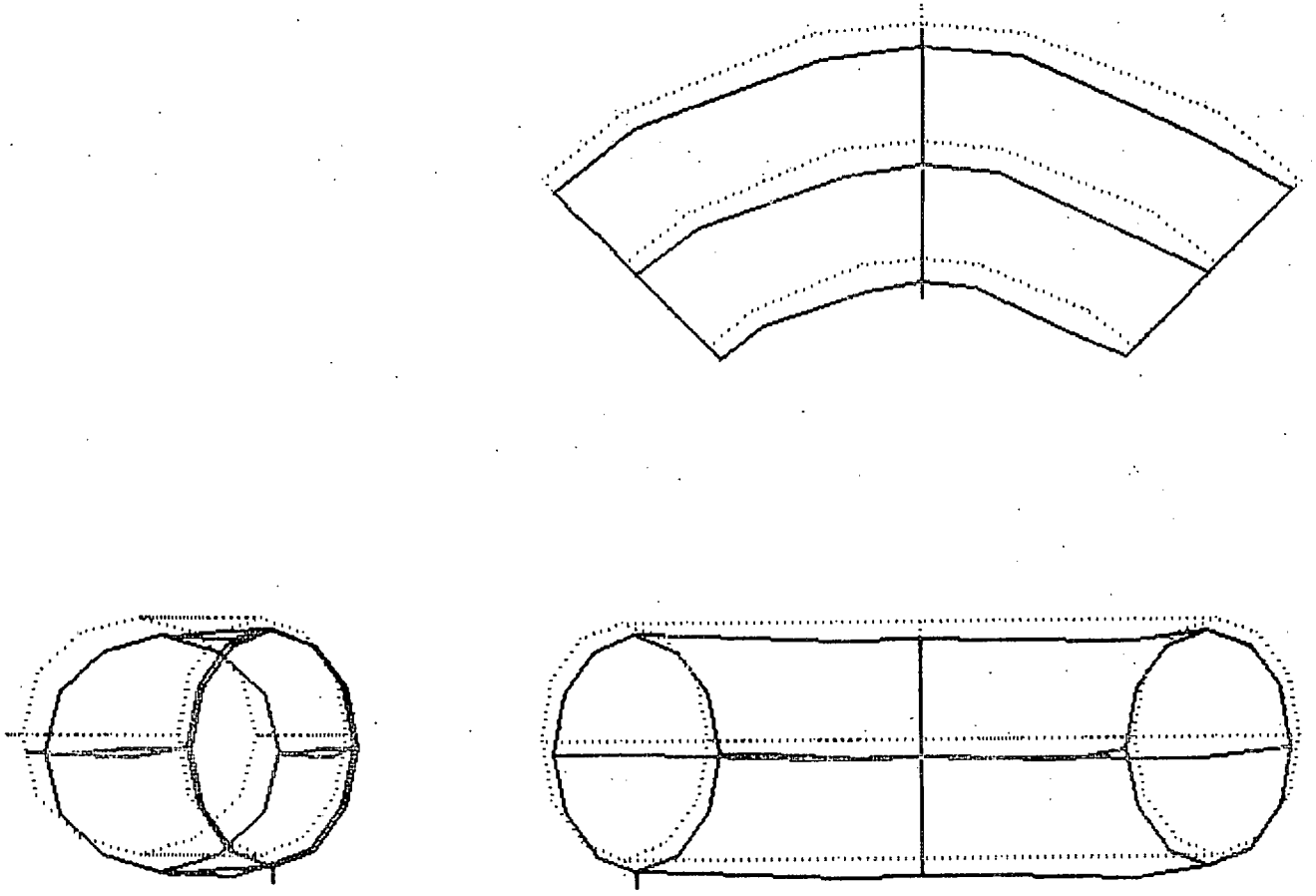

Figure 11 - Mode #4, 13.9 Hz.

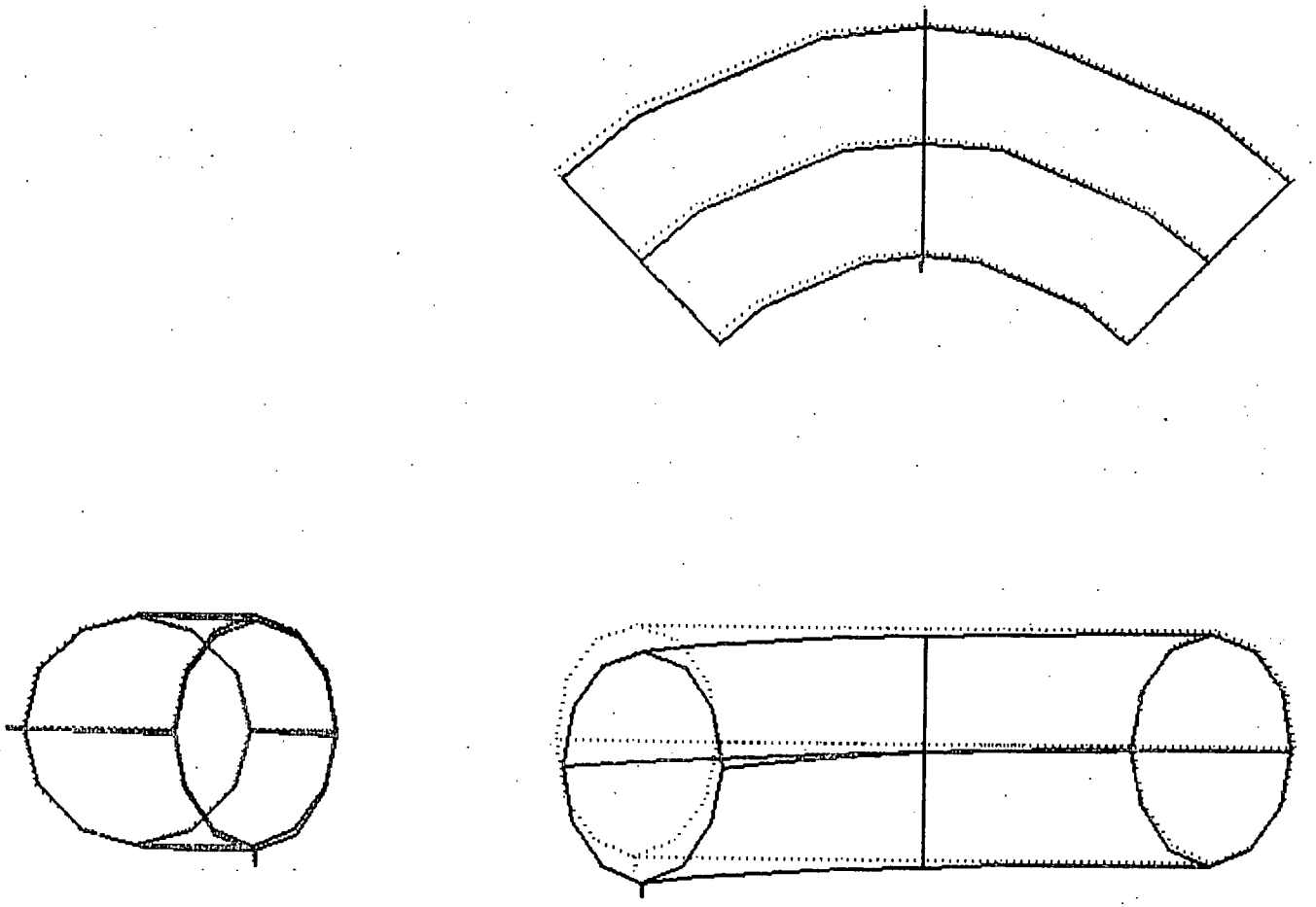

Figure 12 - Mode #5, 25.9 Hz.

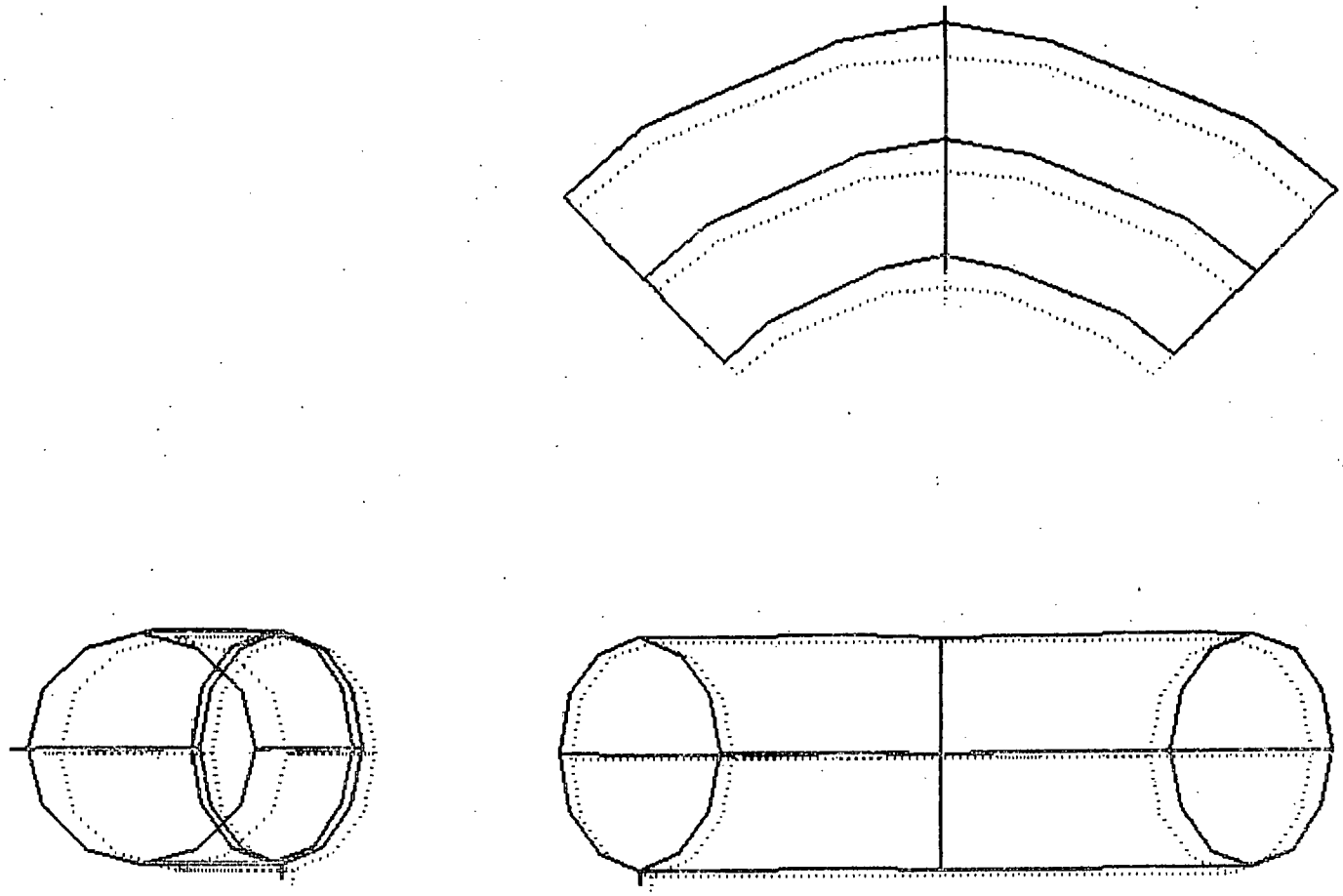

Figure 13 - Mode #6, 59.8 Hz.

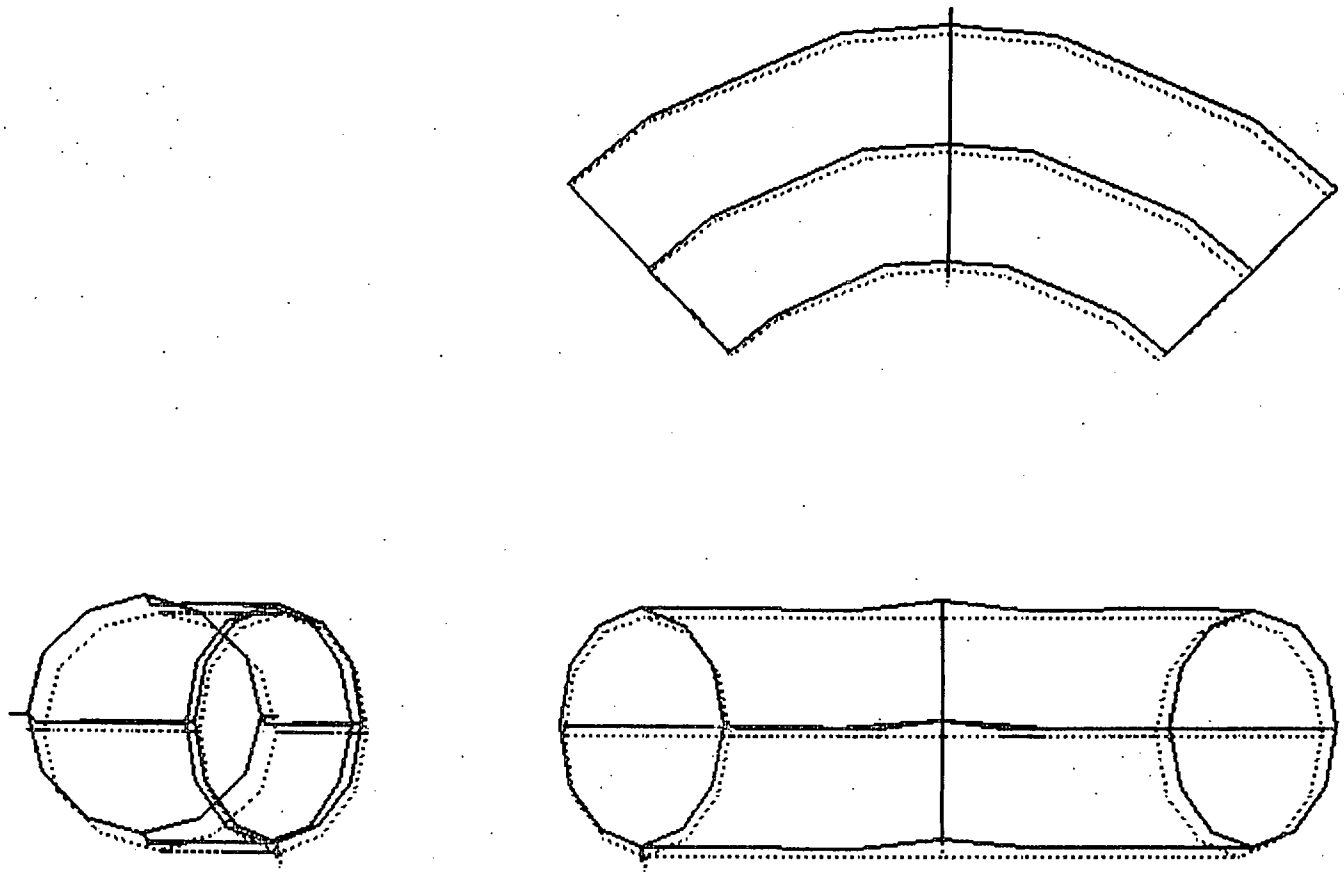

Figure 14 - Mode #7, 61.8 Hz.

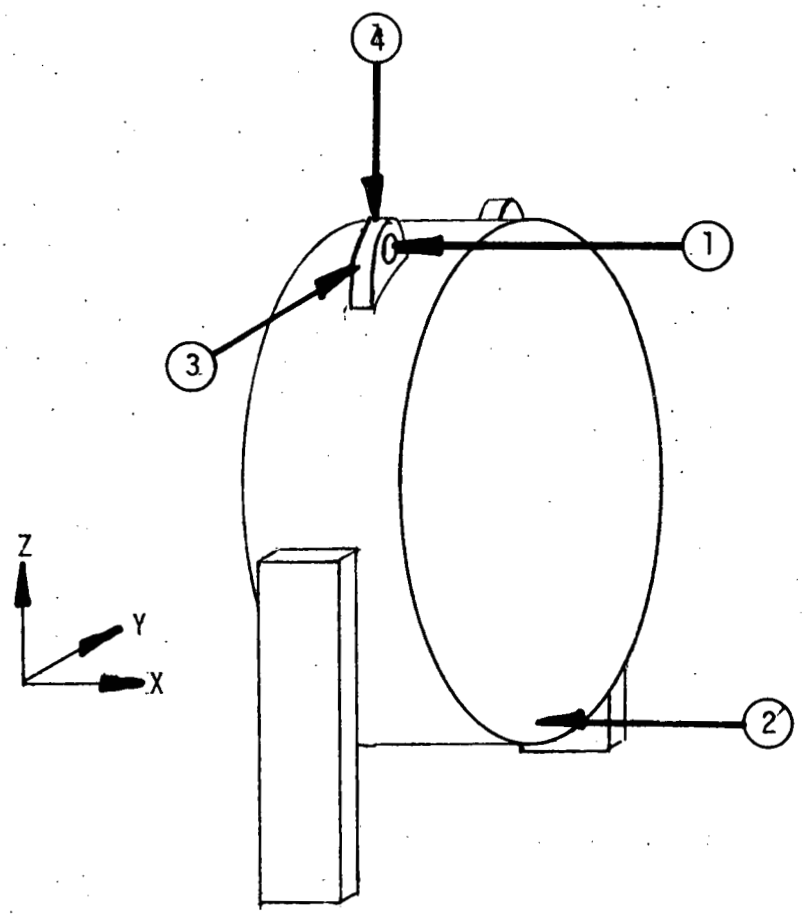

Figure 15 - 7.5° Segment Impact Locations.

Table 2 - 7.5° SEGMENT MODES

Axis	Frequency, Hz	Response Amplitude g Units/Kilonewton
X	9	1.8
X	36	0.28
X	80	0.12
Y	-	-
Z	50	0.012

Printed in the United States of America
Available from
National Technical Information Service
U.S. Department of Commerce
5285 Port Royal Road
Springfield, VA 22161
Price: Printed Copy $; Microfiche $3.00

Page Range	Domestic Price	Page Range	Domestic Price
001–025	$ 3.50	326–350	10.00
026–050	4.00	351–375	10.50
051–075	4.50	376–400	10.75
076–100	5.00	401–425	11.00
101–125	5.50	426–450	11.75
126–150	6.00	451–475	12.00
151–175	6.75	476–500	12.50
176–200	7.50	501–525	12.75
201–225	7.75	526–550	13.00
226–250	8.00	551–575	13.50
251–275	9.00	576–600	13.75
276–300	9.25	601–up	*
301–325	9.75		

*Add $2.50 for each additional 100 page increment from 601 to 1,000 pages; add $4.50 for each additional 100 page increment over 1,000 pages.

Technical Information Department
LAWRENCE LIVERMORE LABORATORY
University of California | Livermore, California | 94550